Riddles, P. W., Blakely, R. L., & Zerner, B. (1970) *Anal. Biochem. 94*, 75–81.
Rosenberry, T. L. (1975) *Adv. Enzymol. Relat. Areas Mol. Biol. 43*, 103–218.
Rotundo, R. L. (1987) in *The Vertebrate Neuromuscular Junction* (Salpeter, M. M., Ed.) Chapter 6, Alan R. Liss, Inc., New York.
Schumacher, M., Camp, S., Maulet, Y., Newton, M., MacPhee-Quigley, K., Taylor, S. S., Friedmann, T., & Taylor, P. (1986) *Nature 319*, 407–409.
Segel, I. H. (1975) *Enzyme Kinetics*, Chapter 4, J. Wiley and Sons, New York.
Taylor, P., & Lappi, S. (1975) *Biochemistry 14*, 1989–1997.
Taylor, P., Jones, J. W., & Jacobs, N. M. (1974) *Mol. Pharmacol. 10*, 78–92.
Tomlinson, G., Mutus, B., & Rutherford, W. J. (1978) *Can. J. Biochem. 56*, 1133–1140.
Tomlinson, G., Mutus, B., & McLennan, I. (1980) *Mol. Pharmacol. 18*, 33–39.
Toutant, J.-P. & Massoulie, J. (1988) in *The Cholinergic Synapse* (Whittaker, V. P., Ed.) Chapter 8b, Springer-Verlag, New York.
Tsuchiya, H., Hayashi, T., Naruse, H., & Takagi, N. (1982) *J. Chromatogr. 234*, 121–130.
Wilson, I. B., & Cabib, E. (1956) *J. Am. Chem. Soc. 78*, 202–207.

Intrinsic Fluorescence of Binding-Site Fragments of the Nicotinic Acetylcholine Receptor: Perturbations Produced upon Binding α-Bungarotoxin†

S. Frieda Pearce and Edward Hawrot*,‡
Department of Pharmacology, Yale University School of Medicine, 333 Cedar Street, New Haven, Connecticut 06510
Received May 14, 1990; Revised Manuscript Received July 27, 1990

ABSTRACT: Synthetic peptides corresponding to sequences contained within residues 173–204 of the α-subunit in the nicotinic acetylcholine receptor (nAChR) of *Torpedo californica* bind the competitive antagonist α-bungarotoxin (BGTX) with relative high affinity. Since the synthetic peptide fragments of the receptor and BGTX each contain a small number of aromatic residues, intrinsic fluorescence studies were used to investigate their interaction. We examined a number of receptor-derived peptide fragments of increasing length (4–32 amino acids). Changes in the λ_{max} and quantum yield with increasing polypeptide chain length suggest an increase in the hydrophobicity of the tryptophan environment. When selective excitation and subtraction were used to reveal the tyrosine fluorescence of the peptides, a significant red shift in emission was observed and was found to be due to an excited-state tyrosinate. The binding of BGTX to the receptor-derived peptide fragments resulted in a large increase in fluorescence. In addition, at equilibrium, the λ_{max} of tryptophan fluorescence was shifted to shorter wavelengths. The fluorescence enhancement, which was saturable with either peptide or BGTX, was used to determine the dissociation constants for the complexes. At pH 7.4, the apparent K_d for a dodecameric peptide (α185–196), consisting of residues 185–196 in the α-subunit of the nAChR from *Torpedo californica*, was 1.4 μM. The K_d for an 18-mer (α181–198), consisting of residues 181–198 of the *Torpedo* α-subunit, was 0.3 μM. No binding or enhanced fluorescence was observed with an irrelevant synthetic peptide of comparable composition. The enhanced fluorescence upon binding was attributable to a change in the environment of the aromatic residues, formation of an excited-state tyrosinate, resonance energy-transfer mechanisms, and a possible reduction in the intrinsic quenching of the tryptophan fluorescence in native BGTX. Trp–Trp energy-transfer calculations suggest that the minimum distance between the tryptophan side chain of the dodecamer (α185–196) and the tryptophan in BGTX is ~12 Å. Distance constraints in this range serve as a useful complement to NOE-derived distance constraints (≤4 Å) obtained from 2D NMR experiments.

The nicotinic acetylcholine receptor (nAChR)[1] mediates signal transduction at the neuromuscular junction by using the binding of acetylcholine to trigger the opening of a cation channel within the receptor. The nAChR is a pentameric array, $\alpha_2\beta\gamma\delta$, of four subunits (Karlin, 1980), where the α-subunit contains the binding site for agonists such as acetylcholine, for α-neurotoxins, and for other competitive antagonists. The binding of competitive antagonists such as the curaremimetic snake toxins (e.g., BGTX) leads to functional blockade of neuromuscular transmission (Changeux et al., 1984). It has been suggested that both agonists and antagonists produce conformational changes in the nAChR upon binding [e.g., see McCarthy & Stroud (1989)]. Many groups have used fluorescence measurements, sensitive to conformational alterations, to study ligand and neurotoxin binding to the nAChR (Weber et al., 1971; Cohen & Changeux, 1975; Eldefrawi & Eldefrawi, 1977; Heidemann & Changeux, 1978). Agonist binding to the nAChR from *Torpedo marmorata* (Bonner et al., 1976; Barrantes, 1978) or from *Narke*

† This work was done during the tenure of an Established Investigatorship from the American Heart Association (E.H.) and was supported by NIH Grants GM32629 and CA09085.
‡ Present address: Section of Molecular and Biochemical Pharmacology, Division of Biology and Medicine, Box G-B487, Brown University, Providence, RI 02912.

[1] Abbreviations: nAChR, nicotinic acetylcholine receptor; BGTX, α-bungarotoxin; *A*, absorbance, *e*, efficiency; R_0, critical transfer distance; *F*, fluorescence; λ_{max}, emission maxima, Φ, quantum yield; λ_{ex}, excitation wavelength; λ_{em}, emission wavelength; Trp, tryptophan; Tyr, tyrosine.

0006-2960/90/0429-10649$02.50/0

japonica (Kaneda et al., 1982), for example, leads to quenching of the intrinsic fluorescence. Snake venom neurotoxin binding to the nAChR can lead to either enhanced fluorescence or quenching depending on the specific α-neurotoxin being examined (Endo et al., 1986). The identity, however, of the specific aromatic residues responsible for the fluorescence perturbations upon binding has not been determined.

The complete understanding of receptor function will depend on the localization within the receptor molecule of structural and functional domains such as the ligand-binding site. Information on the configuration of the binding site could help elucidate the molecular events that lead to ligand-activated channel gating. The snake venom derived, curaremimetic neurotoxins have provided valuable tools for the biochemical and molecular dissection of the nAChR. These toxins bind with extremely high affinity to a region overlapping the acetylcholine binding site (Karlsson, 1979; Karlin, 1980). By use of peptide mapping techniques to localize the neurotoxin binding site on the α-subunit, a number of laboratories have obtained evidence that residues 173–204 on the α-subunit are directly involved in neurotoxin binding (Kao et al., 1984; Wilson et al., 1985; Neumann et al., 1985; Dennis et al., 1986; Oblas et al., 1986; Pederson et al., 1986). A number of synthetic peptides corresponding to sequences within α173–204 have been prepared and have been shown to bind BGTX (Wilson et al., 1985; Neumann et al., 1986a,b; Mulac-Jericevic & Atassi, 1986; Ralston et al., 1987). The binding affinity of these fragments is reduced in comparison to the native nAChR (e.g., apparent K_d of the 32-mer, α173–204, is ~50–100 nM). These synthetic peptide fragments, nevertheless, provide a useful model for the study of the molecular interactions between the receptor's binding site and the α-neurotoxins. Solid-phase binding assays have been used to study toxin binding to several synthetic peptides derived from the *Torpedo* sequence including the dodecamer (α185–196) (Neumann et al., 1986a) and indicate that binding affinity is decreased in peptides shorter than the 32-mer (α173–204) (Ralston et al., 1987; Wilson et al., 1988). A synthetic peptide derived from the sequence of the calf α-subunit (α179–191), however, is reported to retain a toxin-binding affinity similar to that of the intact receptor (Radding et al., 1988). The peptide studies together with recombinant expression of portions of the α-subunit (Barkas et al., 1987; Aronheim et al., 1988) have confirmed that a major determinant of the toxin-binding site is located within the region containing amino acid residues 173–204 of the α-subunit. Agonists also bind to peptides from within this region but with a shift in affinities similar in magnitude to that seen with BGTX (Neumann et al., 1986a; Radding et al., 1988; Fraenkel et al., 1989).

In this paper, we have determined the intrinsic fluorescence characteristics of a number of peptide fragments obtained from within the major determinant of neurotoxin binding. We have also examined the intrinsic fluorescence perturbations produced upon formation of the peptide–BGTX complex. These studies suggest that there are significant changes in the environment of the aromatic residues upon binding. In general, the binding of BGTX to the synthetic peptides examined in this study is accompanied by a large increase in quantum yield. The fluorescence enhancement upon binding was used to determine the binding affinities, in solution, of several of the synthetic peptides. We have also obtained information on the environment of the fluorescent residues within the peptides and their complexes with BGTX, and we have calculated the average distances between the fluorescent residues in the shorter peptides. Preliminary accounts of some of this work have appeared in abstract form (Shi et al., 1988; Pearce & Hawrot, 1989, 1990).

Table I: Sequences of Peptides Used for Fluorescence Studies and Their Relative Positions with Respect to the Primary Sequence of the *Torpedo* α-Subunit[a]

Peptide	175 180 185 190 195 200
32mer (α173-204)	Ac-S G E W V M K D Y R G W K H W V Y Y T C C P D T P Y L D I T Y H - amide
18mer(b) (α181-198)	Ac - Y R G W K H W V Y Y T C C P D T P Y - amide
18mer(u) (α181-198)	Y R G W K H W V Y Y T C C P D T P Y
12mer (dodecamer) (α185-196)	K H W V Y Y T C C P D T
4mer (tetramer) (α187-190)	Ac - W V Y Y - amide
α193-204	C P D T P Y L D I T Y H
Control-14mer	Ac - S T F C L D C V P E T L W E - amide

[a] The control 14-mer sequence is unrelated to the α-subunit; its amino acid composition is similar to that of the dodecamer (α185–196).

Materials and Methods

Synthetic Peptides. Peptides were synthesized by the Protein and Nucleic Acid Chemistry Facility, Yale University, School of Medicine, New Haven, CT, using the sequence from the α-subunit of *Torpedo californica* (Table I). The numbering scheme used to identify the individual peptides is based on the position of the peptide sequence in the primary sequence of the α-subunit. Thus, the 18-mer (α181–198) corresponds to a peptide of 18 residues whose N-terminal amino acid corresponds to position 181 in the α-subunit (see Table I). An irrelevant peptide of 14 residues was used as a control in these studies. The 32-mer (α173–204) and the 4-mer (α187–190) were prepared with blocked termini. The 18-mer (α181–198) was prepared with blocked termini [designated as 18-mer(b)] and with unblocked termini [designated as 18-mer(u)]. The amino acid composition and the concentrations of standard solutions of the peptides were determined by ion-exchange analysis of the performic acid oxidation products on a Beckman Model 6300 amino acid analyzer. All other chemicals used for these studies were obtained from Sigma or Aldrich.

All peptides were completely soluble in aqueous solutions under all pH conditions and peptide concentrations examined in this study. The fluorescence spectra of the peptides at concentrations of up to 25 μM gave no indication of peptide aggregation. There was no change in the overall shape of the spectrum nor was there any concentration-dependent alteration in the λ_{max}. Likewise, circular dichroism studies (unpublished data) of the dodecamer (α185–196) rule out any peptide aggregation in aqueous solutions at peptide concentrations of up to 0.14 mM. In general, the peptides were soluble up to concentrations of about 0.1 mM at neutral pH and up to several millimolar under acidic or basic conditions.

Intrinsic Fluorescence Spectroscopy. Intrinsic fluorescence studies of peptides and BGTX were performed at 22 °C using an SLM-8000 scanning spectrofluorometer equipped with a constant-temperature cuvette holder and an IBM-AT computer for data acquisition. All data collection and analyses were performed with SLM software. Both excitation and emission monochromators were set at 4-nm slit widths. Spectra were obtained with 1-cm quartz cells using excitation wavelengths of 275, 280, or 295 nm as described below. Fluorescence emission was monitored between 290 and 450 nm. Each recorded spectrum was an average of three separate scans. Stock solutions were diluted 24 h prior to analysis to give 1–2 μM samples ($A_{280} \approx 0.02$) which were used for analyses. In all experiments, the fluorescence intensities of

the peptides were linear functions of concentration. The spectra were corrected for variation in the intensity of the excitation source with reference to a Rhodamine quantum counter and were adjusted for Raman emission by buffer subtraction. Tryptophan fluorescence was routinely measured with excitation at 295 nm. Tyrosine emission spectra were obtained by a difference subtraction method as previously described (Weber & Young, 1964; Eisinger, 1969; Kronman & Holmes, 1971; Longworth, 1971; Weinberg, 1988). Spectra obtained with excitation at 295 nm were subtracted from spectra obtained with excitation at 280 nm, after normalization of both spectra at 400 nm, where tyrosine fluorescence is negligible. The fluorescence quantum yield of peptides and BGTX relative to tyrosine and tryptophan was calculated as $(E_s/E_r)(A_r/A_s)$ where E is the area under the complete emission spectrum, A is the absorbance at the wavelength of excitation, s is the sample, and r is an equimolar reference solution of tryptophan or tyrosine. Relative fluorescence quantum yields of tryptophan and tyrosine were calculated by using quinine sulfate as a standard (Parker & Rees, 1966).

Standard tyrosine solutions were prepared by dissolving tyrosine in 0.1 M NaOH. All other samples were maintained at neutral pH in 5 mM phosphate buffer unless pH effects were being studied. Absorption spectra were recorded with a Perkin-Elmer Lambda 6 PECSS system. The ionization constant (pK_a) for tyrosine phenolate was determined spectrophotometrically (Albert & Serjeant, 1971) by using the following equation where the A_{295} of the ionized species (d_I) is greater than the A_{295} of the unionized molecular species (d_M):

$$pK_a = pH + \log (d - d_M)/(d_I - d)$$

and where d is the absorbance at 295 nm obtained at a particular pH.

An excited-state tyrosinate (Szabo et al., 1978) should be revealed by the same difference subtraction procedure used above to determine tyrosine fluorescence (Longworth, 1981; Prendergast et al., 1984). The ionization constant for the excited-state tyrosine phenolate was determined fluorometrically since the fluorescence emission at 335 nm of the ionized species is greater than the fluorescence of the unionized species.

Intramolecular Singlet Excitation Transfer in Peptide Fragments. The 4-mer (WVYY) contains a major fraction of the aromatic residues found in the larger peptides that bind BGTX (Table I). Due to their proximity in space, it is likely that there is energy transfer from the tyrosine to tryptophan. In this relatively simple case, the average distance between the two tyrosines and tryptophan can be calculated from the efficiency of transfer (Förster, 1966). In the longer peptides (Table I), there are up to five tyrosines and three tryptophans with the possibility for both tyrosine to tryptophan and Trp to Trp energy transfer. Calculation of distances in these cases gives the average distance between each pair of donor–acceptor chromophore groups (i.e., Tyr–Trp, Trp–Trp).

The quantum yield [$Q(\lambda)$ at wavelength λ] of a protein containing tryptophan and tyrosine (neglecting the minor contribution of phenylalanine) is represented by

$$Q(\lambda) = Q_T[f_{Trp}(\lambda) + ef_{Tyr}(\lambda)]$$

where Q_T is the quantum yield of tryptophan in the protein and $f_{Trp}(\lambda)$ and $f_{Tyr}(\lambda)$ are the fractional absorbance by tryptophan and tyrosine residues at wavelength (λ) and e is the efficiency of energy transfer from tyrosine to tryptophan residues. As only the wavelength dependence of the quantum yield is required (Saito et al., 1981), the absolute values of quantum yields are not necessary. The analysis of the wavelength dependence of the relative tryptophan quantum yield was used to determine the efficiency of tyrosine to tryptophan energy transfer (Eisinger et al., 1969; Saito et al., 1981; Weinberg, 1988) as indicated in the equation:

$$[I(\lambda)/A(\lambda)]/(I_{295}/A_{295}) = (1 - e)f_{Trp}(\lambda) + e$$

where $I(\gamma)$ is the fluorescence intensity at a given wavelength, and $A(\lambda)$ is the optical density of the solution measured at the same wavelength (Saito et al., 1981). Energy transfer in the peptides and peptide–BGTX complexes was measured in phosphate buffer at pH 7.4. The fractional absorbance of tryptophan in the peptides was determined by multiplying the total A_{280} by the fractional absorbance of tryptophan obtained from a standard solution of tyrosine and tryptophan adjusted to the ratio present in the peptide.

The Förster distance, R_0, together with the determination of e can be used to calculate intramolecular distances in proteins (Förster, 1966). The efficiency of transfer between a donor and acceptor, separated by a distance r, becomes half when $r = R_0$:

$$r = (e^{-1} - 1)^{1/6}R_0$$

In this equation, e is the efficiency of energy transfer and r is the distance between two identified chromophores where R_0 defines, for each possible donor and acceptor pair, the distance at which the transfer rate equals the donor decay rate. The value of R_0 may be calculated from the relationship:

$$R_0^6 = (8.8 \times 10^{-25})\kappa^2\Phi_D n^{-4} J_{AD}$$

The value for $\langle\kappa^2\rangle_{av}$ was taken as $^2/_3$ assuming that the chromophores are free to rotate at a rate which is much greater than the deexcitation rate of the donor (Förster 1966). In water, the value for the index of refraction, n, is 1.4 (Fairclough & Cantor, 1978). The donor quantum yield (Φ_D) for tyrosine was obtained from a peptide containing two tyrosines and no tryptophan (Table I), and the donor quantum yield (Φ_D) for tryptophan was obtained from an unrelated short peptide lacking tyrosine (STFCKDCVPETLWE). The spectral overlap integral, J_{AD}, of the donor fluorescence and acceptor absorbance was approximated graphically by the equation (Tao et al., 1983):

$$J_{AD} = \int F_D(\lambda)\epsilon(\lambda)\lambda^4\, d\lambda / \int F_D(\lambda)\, d\lambda$$

where the summation was carried out over 5-nm intervals and where $F_D(\lambda)$ is the fraction of the total donor fluorescence occurring at each λ and $\epsilon(\lambda)$ is the molar decadic absorption coefficient of the acceptor at each λ.

Fluorescence Assay of BGTX Binding to Receptor-Derived Peptide Fragments. The intrinsic fluorescence of defined mixtures of BGTX and synthetic peptides was measured as described above for the peptides alone. In order to use the fluorescence assay to determined the binding constant for the interaction, aliquots of peptides in concentrations ranging from 0.1 nM to 25 μM were added to a solution of 1 μM BGTX in 5 mM phosphate buffer, pH 7.2, unless indicated otherwise, and the corresponding fluorescence (λ_{ex} 280 nm) for each mixture was recorded. The fluorescence spectrum was corrected for (1) Raman scattering of the buffer, (2) the intrinsic fluorescence of the peptide, and (3) the intrinsic fluorescence of BGTX. At concentrations exceeding 20 μM, corrections for inner filter effects were necessary (Saito et al., 1981). The binding data were analyzed by using the program ENZFITTER (Elsevier Publishing Co.) to yield the best-fit hyperbolic binding curve and to estimate the apparent K_d for binding by using the equation:

$$\Delta F/\Delta F_{max} = L/(L + K_d)$$

L is the concentration of added peptide. In some experiments, the concentration of BGTX was varied while holding the peptide concentration constant at 1 μM. Similar K_d values were obtained with either procedure.

Second-Derivative Absorption Spectra. Previous studies have shown that information on the environment of tyrosine residues within polypeptides can be determined by using second-derivative spectroscopy (Ragone et al., 1984). This method is based on differential solvent effects on the absorbance of tyrosine (Donovan, 1969; Ragone et al., 1984). All absorption spectra were recorded on an SLM DW-2000 equipped with an electronic second-derivative accessory. The degree of tyrosine exposure to the solvent (α) was calculated by using the equation:

$$\alpha = (r_n - r_a)/(r_u - r_a)$$

In this equation, r represents a ratio (b/c) of spectral measurements where b represents the peak to trough distance between the second-derivative minimum near 283 nm and the maximum near 287 nm and c is the peak to trough distance between the minimum near 291 nm and the maximum near 295 nm. The subscripts n and u refer to the ratios determined for the native and denatured samples, respectively, and the subscript a refers to a reference mixture containing the same molar ratio of aromatic amino acids as in the sample. The values for r_a, which corresponds to the ratios of tyrosine to tryptophan present in the peptides, are taken from Ragone et al. (1984). Since the absorption of all samples was kept below 0.2, turbidity corrections were not necessary.

Results

The primary amino acid sequences of the nAChR-derived peptide fragments which bind BGTX show a high content of aromatic residues (Wilson et al., 1985). This observation, together with the fact that BGTX contains a single evolutionarily conserved tryptophan, suggested that intrinsic fluorescence measurements may prove useful in studying the mechanism underlying toxin binding. To properly assess the fluorescence changes associated with binding to BGTX, it was first necessary to analyze the intrinsic fluorescence properties of the individual peptides. These observations could then be compared with the intrinsic fluorescence obtained from the complex formed between these peptides and BGTX. In this study, we have focused on a number of small synthetic peptides (Table I) derived from the region in the α-subunit of the nAChR forming the major determinant of the BGTX-binding site. All of the receptor-derived peptide fragments except for the 4-mer (α187–190), WVYY, have affinities for BGTX in the micromolar to submicromolar range (Wilson et al., 1988).

Intrinsic Fluorescence of Peptides. The dodecamer (α185–196), 18-mer(b) (α181–198), 18-mer(u) (α181–198), and 32-mer (α173–204) (Table I) share a core aromatic segment of four residues, WVYY (Table I). We decided to prepare a peptide with this sequence (WVYY) to serve as a model for investigating the fluorescence behavior and energy-transfer properties (see below) of this peptide series. Since the longer peptides contain additional aromatic residues, the fluorescence behavior of the 4-mer (α187–190) facilitates the interpretation of the more complex spectra obtained from these other peptides.

The fluorescence emission spectra (λ_{ex} 280 nm) of these peptides are shown in Figure 1. Since the fluorescence emission spectrum of these peptides is dominated by tryptophan, the spectra are normalized for tryptophan content as shown in Figure 1b. The λ_{max} of the 4-mer (α187–190) is

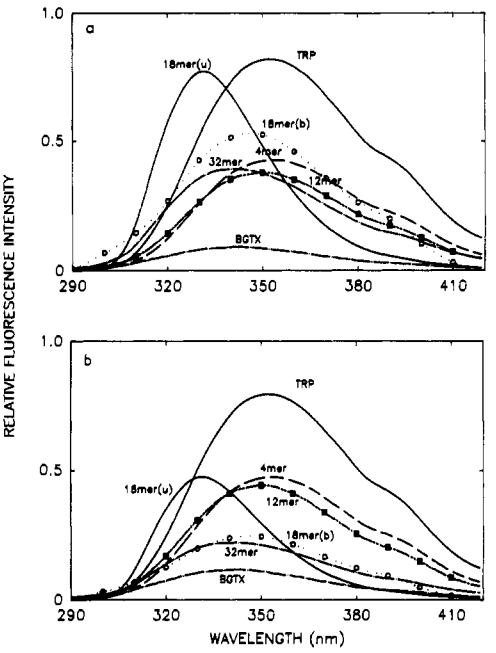

FIGURE 1: Tryptophan fluorescence characteristics of nAChR-derived peptide fragments. (a) Fluorescence emission of 1 μM solutions of the 4-mer (α187–190) (WVYY), dodecamer (α185–196) (KHWVYYTCCPDT), 18-mer (α181–198) (YRGWKHWVYYTCCPDTPY), 32-mer (α173–204), and BGTX at pH 7.4 in 5 mM sodium phosphate buffer. 18-mer(b) refers to 18-mer that is N- and C-terminal blocked; 18-mer(u) refers to 18-mer with unblocked termini. (b) Intrinsic fluorescence normalized per tryptophan residue. The observed emission maxima are as follow: tryptophan, 350 nm; 4-mer (α187–190), 350 nm; dodecamer (α185–196), 350 nm; 18-mer(b) (α181–198), 348 nm; 18-mer(u) (α181–198), 333 nm; 32-mer (α173–204), 342 nm; BGTX, 342 nm.

identical with that of tryptophan in aqueous solution (λ_{max} = 350 nm). With increasing peptide chain length, the emission maxima shift to shorter wavelengths (Table II). The largest shift in λ_{max} was obtained with the 18-mer(u) (α181–198). In contrast, the λ_{max} of the blocked 18-mer(b) (α181–198) was not dramatically shifted, and the quantum yield was significantly lower than that of 18-mer(u) (α181–198) (Table II). Thus, blocking the terminal residue charges by acetylation and amidation produces a large effect on the fluorescence properties of the 18-mer (α181–198) peptide. At pH 3, however, the quantum yield and λ_{max} characteristics of 18-mer(u) (α181–198) are similar to 18-mer(b) (α181–198) measured at either pH 3 or pH 7.4. The decrease in quantum yield with increasing chain length is consistent with the observation that peptide bonds decrease the fluorescence of tyrosine and tryptophan (Cowgill, 1963). It is also noteworthy that BGTX has an unusually low quantum yield in comparison to other proteins [e.g., Φ = 0.08 for adrenocorticotropin (Eisinger, 1969)] and neurotoxins (Chicheportiche et al., 1972).

The tyrosine fluorescence emission spectra (Figure 2) were obtained by selective excitation and subtraction as described under Materials and Methods. As in the case of other proteins where tyrosine fluorescence is detectable, the λ_{max} for tyrosine emission in BGTX is around 310 nm as is the λ_{max} for 18-mer(b) (Table II). In contrast, the other four peptides [4-mer (α187–190), dodecamer (α185–196), 18-mer(u) (α181–198), and 32-mer (α173–204)] show a red-shifted λ_{max}. In the case of the 4-mer (α187–190), there are also significant shoulders at 310 and 325 nm. In general, the quantum yield for tyrosine appears to decrease with increasing chain length. Since the red-shifted tyrosine fluorescence could be due to (1) a ground-state tyrosinate, (2) an excited-state tyrosinate, (3) bityrosine formation, or (4) tyrosine excimer formation, we

Table II: Quantum Yield of Tyrosine and Tryptophan in Peptides and Peptide–BGTX Complexes[a]

peptides	$\Phi_{TOT(280)}$[b]	$\Phi_{Trp(295)}$[c]	$\lambda_{max(Trp)}$ (nm)	Φ_{Tyr}[d]	$\lambda_{max(Tyr)}$ (nm)[e]
4-mer	0.1	0.094	350	0.045	340, 325
12-mer	0.094	0.092	348	0.002	330
18-mer(b)	0.06	0.05	348	0.036	310
18-mer(b), pH 3	0.056	0.048	348	0.035	310
18-mer(u)	0.092	0.086	332	0.025	330
18-mer(u), pH 3	0.05	0.045	342	0.005	310, 325
32-mer	0.056	0.049	342	0.009	334
BGTX	0.04	0.036	342	0.004	310, 323
12-mer + BGTX	0.14	0.13	345	0.02	330, 310
18-mer(b) + BGTX	0.12	0.09	342	0.044	330, 310
18-mer(u) + BGTX	0.18	0.126	330	0.055	329
32-mer + BGTX	0.065	0.059	340	0.009	335, 316

[a] Measurements were carried out in 5 mM phosphate at pH 7.4 unless stated otherwise. [b] Relative quantum yield was normalized with the absorbance measured at 280 nm. [c] Quantum yield was calculated by using 1 μM solutions of peptide and equivalent concentrations of free tryptophan. [d] Quantum yield of tyrosine, including the contribution from tyrosinate, was determined by selective excitation and normalization using 1 μM solutions of peptide and equivalent concentrations of free tyrosine. [e] Fluorescence maxima were obtained by selective excitation and normalization. The second wavelength represents the position of any prominent secondary peak.

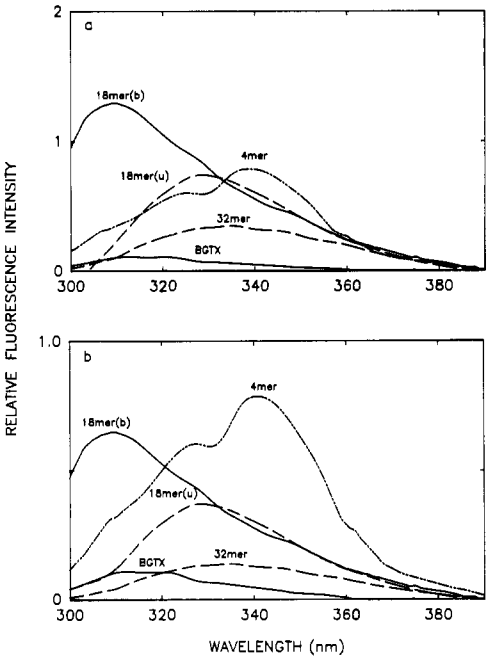

FIGURE 2: Tyrosine fluorescence in nAChR-derived peptide fragments. Tyrosine fluorescence was obtained by differential excitation and subtraction as described under Materials and Methods. (a) Fluorescence emission of 1 μM solutions of the same peptides examined in Figure 1. (b) Fluorescence normalized with respect to tyrosine content. The 18-mer(b) (α181–198) and BGTX each show a λ_{max} around 310 nm, comparable to that of free tyrosine in the same buffer. The 4-mer has a major peak at 340 nm with shoulders at 305 and 330 nm; the 18-mer(u) (α181–198) and 32-mer (α173–204) each have maxima at 330–335 nm. The dodecamer (α185–196) did not show significant tyrosine fluorescence. All measurements were carried out at pH 7.4 in 5 mM sodium phosphate buffer.

examined the pH and denaturant sensitivity of the absorbance and fluorescence properties of these peptides to distinguish among these possibilities. Since ionized phenolic tyrosinate has an absorbance maximum at 295 nm, we measured the

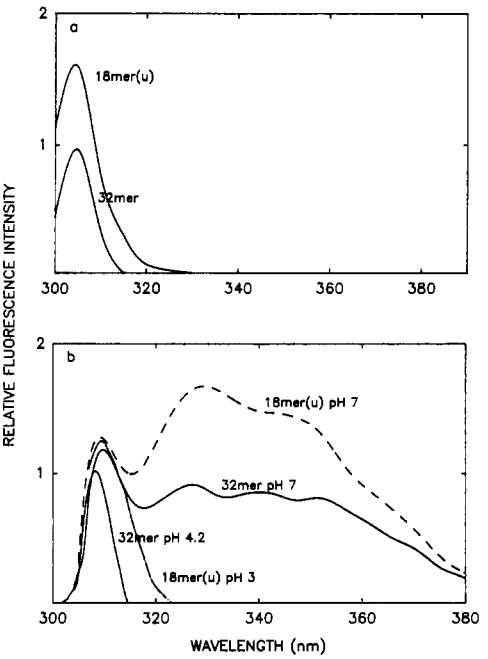

FIGURE 3: Effect of pH and treatment with guanidine hydrochloride on the tyrosine fluorescence of 18-mer(u) (α181–198) and 32-mer (α173–204). (a) In 6 M guanidine hydrochloride, the longer wavelength contributions (Figure 2) are abolished, and a single λ_{max} is obtained near 305 nm. (b) At pH 7, in contrast to pH 7.4 (Figure 2), multiple peaks of tyrosine fluorescence are clearly observed. A major new peak appears with a λ_{max} near 310 nm. At pH <4.2, the fluorescence with λ_{max} at 310 nm predominates, and the longer wavelength fluorescence is abolished.

pK_a's for these peptides. In each case, the phenolic tyrosinate pK_a's appear to be in the normal range of 9–11 based on absorbance measurements at 280 and 295 nm. These observations, clearly showing the lack of any strongly absorbing component at 295 nm at pH values below 10, indicate that a ground-state tyrosinate is not responsible for the red-shifted fluorescence. Similarly, the absence of a longer wavelength absorbance at >290 nm rules out the possibility that tyrosine excimer formation is responsible for the observed fluorescence (Birks, 1970). To address the involvement of covalent di-tyrosine formation (Malencik & Anderson, 1987) we examined the peptides under denaturing conditions. As shown in Figure 3a, incubation of the peptides in 6 M guanidine completely abolishes the red-shifted tyrosine fluorescence and thus eliminates the possible involvement of bityrosine (Lehrer & Fasman, 1967). This observation also rules out the presence of an interfering fluorescent contaminant. The elimination of the red-shifted fluorescence by denaturation is, however, what would be expected if the fluorescence were due to an excited-state tyrosinate (Prendergast et al., 1984). The pK_a of an excited-state tyrosine is generally shifted to much lower pH values in comparison to ground-state tyrosine (Becker, 1969). Consistent with this interpretation, we found that the red-shifted tyrosine fluorescence was pH dependent and, in the case of the 18-mer(u) (α181–198), exhibited an apparent pK_a of 4.2 (Figure 3b). Similarly, the pK_a for the tyrosinate-like fluorescence of the 32-mer (α173–204) was 5.4 (Figure 3b). In both cases, the pH dependence of the red-shifted tyrosine fluorescence was determined with excitation at 280 nm.

In addition, we observed an isotope effect on the red-shifted tyrosine fluorescence. With as little as 25% D_2O added to the peptide solution, the red-shifted tyrosine fluorescence was abolished and converted to a more typical tyrosine emission with a λ_{max} at 310 nm. Since ion transfer is expected to be slower for a deuterium than for a proton (Stryer, 1966), the

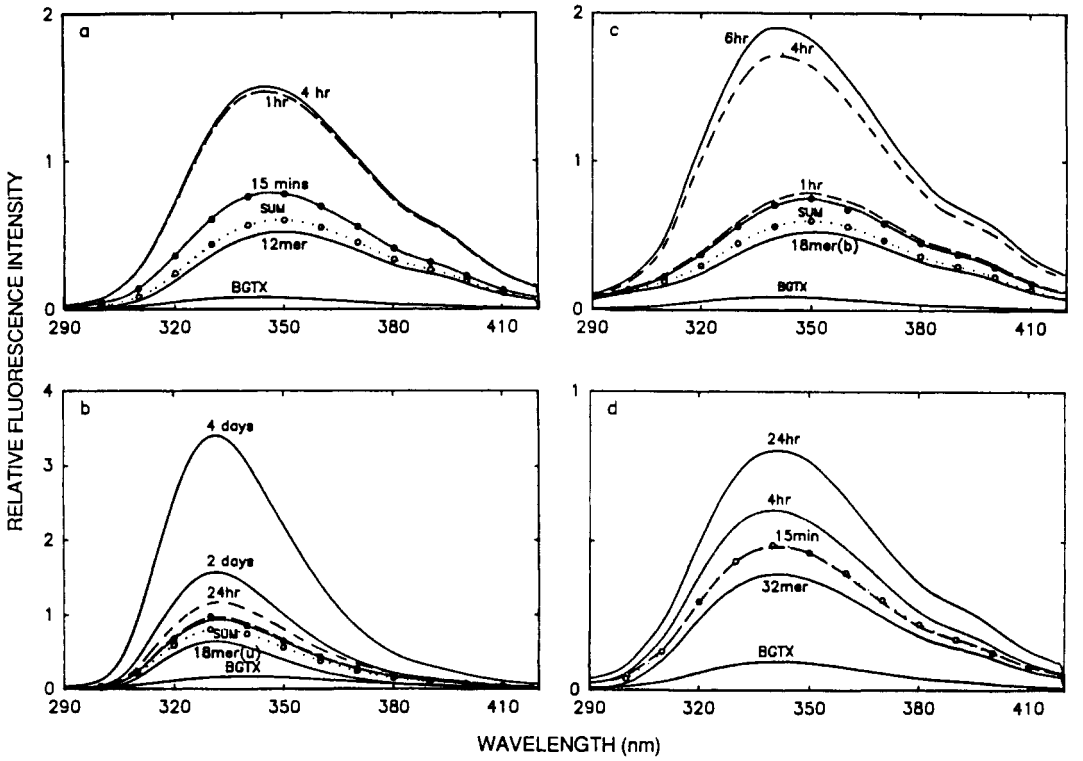

FIGURE 4: Fluorescence spectra upon addition of BGTX to nAChR-derived peptide fragments. Equal volumes of BGTX (1 μM) and peptide (1 μM) were mixed, and the fluorescence emission with λ_{ex} = 280 nm was monitored over time. All solutions contained 5 mM sodium phosphate buffer, pH 7.4. (a) The binding of the dodecamer (α185–196) to BGTX is accompanied by an immediate enhancement of fluorescence. (b) The binding of 18-mer(u) (α181–198) to BGTX produces a steady increase in fluorescence enhancement for a period of 4 days. At equilibrium, there is a corresponding blue shift of the λ_{max} to 330 nm. (c) The binding of 18-mer(b) (α181–198) to BGTX is accompanied initially by a small increase in fluorescence, and after a lag time of about 4 h, the net increase is similar to that observed with the dodecamer (α185–196). The final form of the complex at 6 h exhibits a λ_{max} of 342 nm. (d) The binding of 32-mer (α173–204) to BGTX is also accompanied by a small enhancement of fluorescence. The λ_{max} of this complex is 340 nm at equilibrium. In all cases, (O···O) indicates the calculated sum of the individual spectra obtained for peptide and BGTX; (●—●) corresponds to the 15-min time point for the mixture.

production of an excited-state tyrosinate anion would be hindered in D_2O. In combination, these results strongly suggest that the tyrosinate anion does not exist in the ground state of these peptides but that the observed red-shifted fluorescence is due to proton abstraction in the excited state.

Energy Transfer within the Peptide Sequences. The relative quantum yield of the tyrosine fluorescence in a related peptide (α193–204) (Table I) lacking tryptophan has a value of 0.06. In general, the tyrosine fluorescence quantum yield in the peptide fragments and in BGTX appears to be reduced (quantum yield of Tyr = 0.002–0.036), suggestive of quenching of the tyrosine fluorescence possibly through intramolecular energy transfer from tyrosine to tryptophan. Assuming that in these relatively short polypeptides energy transfer from tyrosine to tryptophan is largely responsible for the observed quenching of tyrosine fluorescence, we calculated the Förster R_0 distance for this pair of aromatic amino acids in order to obtain some approximate intramolecular distance constraint. Calculations of J_{AD} and R_0 (Table III) for various pairs of chromophores were based on Φ_d = 0.1 for tryptophan and 0.06 for tyrosine. Since the calculated distance R_0 is sensitive to red shifts in the emission spectrum (Stryer, 1978), the actual distance r between chromophores can be obtained from R_0 and measurements of the efficiency of energy transfer (e) as described under Materials and Methods. Such analyses are easily interpretable for single pairs of chromophores. When there are more than two chromophores, however, the calculated distances represent an average transfer distance between donor and acceptor groups of chromophores.

In the simplest peptide, the 4-mer (α187–190), the effective average distance r between the two adjacent tyrosine residues and the single tryptophan is 6.9 Å (Table III), consistent with molecular modeling of distances within this sequence. In the longer peptides, the effective average distance between tyrosine and tryptophan groups remains unchanged except for the 18-mer(b) (α181–198) where r = 11.7 Å. The difference in distance r between 18-mer(b) (α181–198) and 18-mer(u) (α181–198) is consistent with the difference in the tyrosine fluorescence (λ_{max} and Φ_{Tyr}) observed for these two peptides and suggests a difference in their conformations. The distances calculated from intramolecular energy transfer serve as a base line for similar analysis of the bound complexes.

Fluorescence of Peptide–BGTX Complexes. Addition of the peptides [dodecamer (α185–196), 18-mers (α181–198), and 32-mer (α173–204)] to BGTX is accompanied by a large increase in fluorescence which exceeds the total fluorescence expected from the summation of peptide and BGTX fluorescence spectra (Figure 4). At equilibrium, the enhanced fluorescence is accompanied by a significant blue shift of the tryptophan λ_{max} suggestive of an increase in the hydrophobic environment of tryptophan. With several of the peptides, the time course for binding was slow, ranging from 1 to 100 h (Figure 5). There was no apparent degradation or proteolysis over this entire time of incubation. In general, we also observed that the initial rate of appearance of the tryptophan fluorescence enhancement decreased with increasing temperature in the range from 25 to 40 °C (unpublished results).

In order to examine the specificity of binding in the fluorescence assay, a tryptophan-containing peptide of unrelated sequence (control 14-mer) (Table I) was used to determine the level of nonspecific interaction. At all concentrations examined, the fluorescence spectrum for a mixture

Table III: Calculation of Overlap Integrals (J_{AD}) and Effective Average Distance (r)[a]

peptides	donor	acceptor	$J_{AD} \times 10^{-16}$ M^{-1} cm^{-6}	R_0 (Å)	e	r (Å)
4-mer	Tyr$^-$	Trp	0.32	7.7	0.66	6.9
12-mer	Tyr$^-$	Trp	0.2	7.1	0.8	6.6
18-mer (b)	Tyr	Trp	2.4	10.6	0.4	11.7
18-mer(u)	Tyr$^-$	Trp	0.45	8.1	0.6	7.6
18-mer(u)	Trp	Trp	8.7	14.3		
32-mer	Tyr$^-$	Trp	0.55	8.4	0.85	7.6
BGTX	Tyr	Trp	2.8	11.8	0.33	13.3[b]
12-mer + BGTX	Trp	Trp	2.4	11.5		
18-mer(b) + BGTX	Trp	Trp	3.6	12.5		
18-mer(u) + BGTX	Trp	Trp	9.7	14.8		
32-mer + BGTX	Trp	Trp	3.8	12.6		
12-mer + BGTX	Tyr$^-$	Trp	0.54	8.4	0.6	7.8
18-mer(b) + BGTX	Tyr$^-$	Trp	0.74	8.7	0.3	9.9
18-mer(u) + BGTX	Tyr$^-$	Trp	0.45	8.1	0.3	9.3
32-mer + BGTX	Tyr$^-$	Trp	0.3	7.5	0.5	7.5

[a] R_0 is the characteristic transfer distance for singlet transfer between pairs of chromophores and is calculated from the overlap integral J_{AD} as discussed under Materials and Methods. The effective average distance r between any two chromophores, when there are multiple donor–acceptor pairs, was calculated from R_0 and from the efficiency e value as described under Materials and Methods. The parameter κ^2 was set at $^2/_3$. If κ^2 were set at 0.475, assuming a relative motion of acceptor and donor that is slow compared to donor lifetime (Maksimov & Rozman, 1968; Steinberg, 1968), the values of the calculated R_0 would be decreased by 0.7 Å. [b] The distance obtained for Tyr–Trp distance in BGTX is in good agreement with the value of 13 Å reported in the literature (Menez et al., 1980).

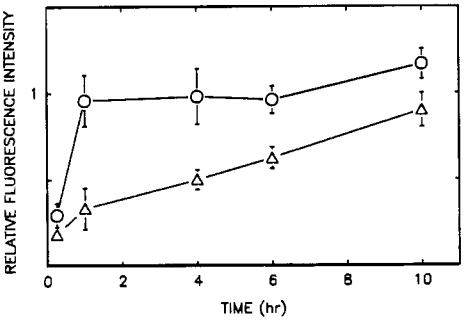

FIGURE 5: Time course of fluorescence enhancement observed with BGTX binding to the dodecamer (α185–196) and 18-mer(u) (α181–198). The data in Figure 4 are replotted to show the net increase in fluorescence upon complex formation. (O) corresponds to the dodecamer (α185–196) complex, and (Δ) is the 18-mer(u) (α181–198) complex. The dodecamer (α185–196) shows an immediate enhancement of fluorescence which is maintained for at least 24 h. In contrast, the fluorescence enhancement observed with the 18-mer(u) (α181–198) increases slowly over a period of several days.

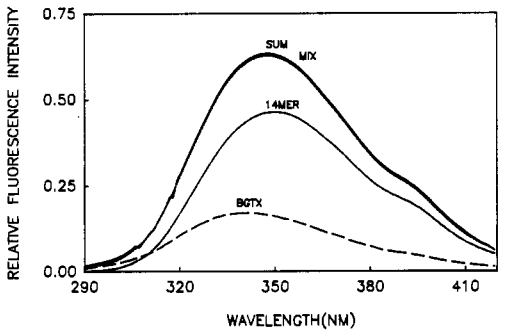

FIGURE 6: Fluorescence spectra upon addition of BGTX to an irrelevant peptide. An irrelevant peptide (14-mer) with an amino acid composition similar to that of the nAChR-derived peptide fragments was used as a control (Table I). The fluorescence of the 1:1 mixture of this 14-mer and BGTX is exactly equal to the sum of the individual spectra for BGTX and for the 14-mer. No fluorescence enhancement is observed.

of BGTX and the control 14-mer peptide was exactly identical with the addition of the spectra of the two components (Figure 6), thus ruling out any nonspecific interactions in this range of concentrations.

As was seen with many of the peptides alone (Figure 2), the complexes of peptides and BGTX have a demonstrable red-shifted tyrosine fluorescence with a λ_{max} of 330 nm (Figure 7). The λ_{max} of the complex formed between BGTX and 18-mer(b) (α181–198) was also shifted to 330 nm, in line with the other complexes, even though this peptide did not normally exhibit a red-shifted tyrosine fluorescence. Thus, an excited-state tyrosinate appears to be a common feature for all the complexes.

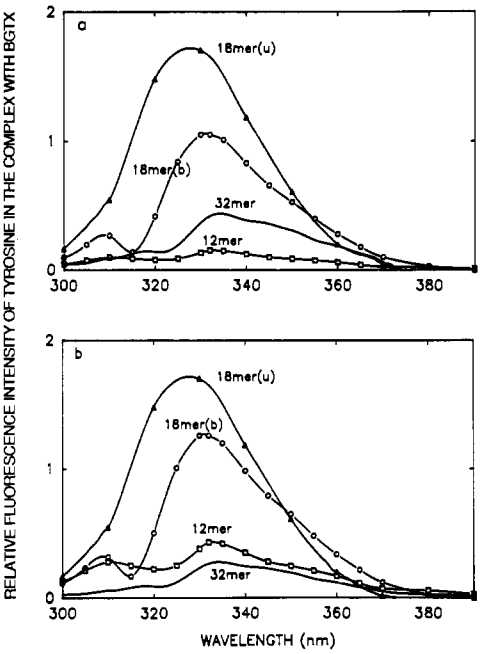

FIGURE 7: Tyrosine fluorescence emission spectra observed in the peptide–BGTX complexes. The tyrosine fluorescence spectra were obtained as described under Materials and Methods. (a) Tyrosine fluorescence spectra for 1:1 mixtures of BGTX and the indicated peptides were determined at a final concentration of 0.5 μM BGTX in 5 mM sodium phosphate buffer at pH 7.4. (b) The fluorescence spectra in (a) were normalized with respect to tyrosine content. The dodecamer (α185–196) complex has a λ_{max} of 330 nm with a secondary peak at 310 nm. The 18-mer(b) (α181–198) complex has a major peak at 330 nm and a minor one at 310 nm. The 18-mer(u) (α181–198) complex has a single peak at 329 nm while the 32-mer (α173–204) has a relatively broad peak at 335 nm extending to longer wavelengths.

Equilibrium Dissociation Constants. The fluorescence enhancement produced upon binding of peptides to BGTX was used to determine the dissociation constant in solution. Typically, varying amounts of the synthetic peptides [dodecamer (α185–196) or 18-mer (α181–198); concentrations

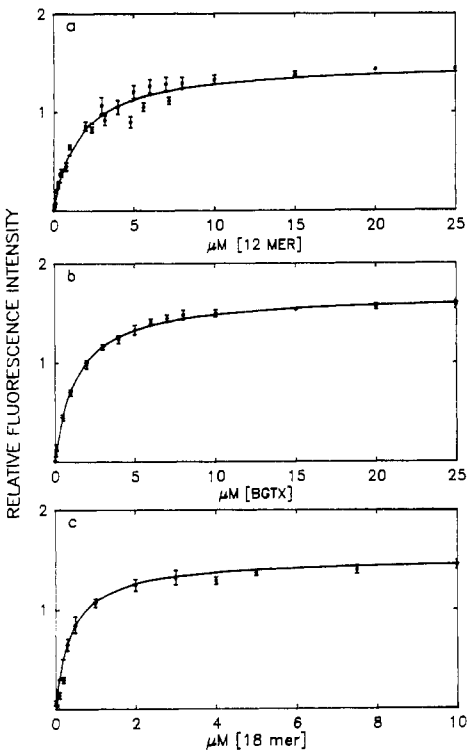

FIGURE 8: Concentration dependence of fluorescence enhancement. (a) Net fluorescence enhancement upon binding of the dodecamer (α185–196) to BGTX at pH 7.0 is saturable with respect to added dodecamer. The final BGTX concentration was 1 μM in each sample. The calculated dissociation constant was 1.44 ± 0.28 μM at pH 7.0 in 5 mM sodium phosphate buffer. (b) Fluorescence enhancement is saturable with respect to added BGTX. The final concentration of the dodecamer (α185–196) was held at 1 μM. The calculated K_d was 1.1 μM. (c) The fluorescence enhancement upon addition of BGTX to 18-mer(u) (α181–198) was saturable with respect to peptide and yielded a K_d of 0.33 ± 0.05 μM.

ranging from 0.1 to 100 μM] were added to a given concentration of BGTX. The net increase in fluorescence was determined as described under Materials and Methods, after appropriate correction for the intrinsic fluorescence due to BGTX and peptide, and was found to be saturable with respect to peptide (Figure 8). The apparent dissociation constants were calculated by assuming a single-site interaction. The binding constants were 1.4 μM for the dodecamer (α185–196), 0.8 μM for the 18-mer(b) (α181–198), and 0.33 μM for the 18-mer(u) (α181–198) (Figure 8). Similar results were obtained when the peptide concentration was held constant and the concentration of BGTX was varied. To examine the pH dependence of binding, binding studies with the dodecamer (α185–196) were carried out at pH 3, 5, 7.4, and 9. The apparent K_d was close to 1 μM at all four pH values.

Energy Transfer in the Peptide–BGTX Complexes. Since energy-transfer mechanisms often contribute to observed increases in fluorescence quantum yield, we wanted to calculate effective average distances between donor and acceptor groups of chromophores that may be responsible for such fluorescence increases. Table III lists the calculated average distance (r) for tyrosine to tryptophan and Trp to Trp transfer in the complexes of BGTX and peptides. The average distance (r) between the sole tryptophan in BGTX (Trp-28) and the single tryptophan (Trp-187) in the dodecamer (α185–196) was calculated to be no closer than 11.5 Å (Table III) assuming for the sake of this calculation that all of the fluorescence enhancement was due to Trp–Trp energy transfer. In the case of the 18-mer(u) (α181–198) which contains an additional tryptophan, the apparent Trp–Trp distance separation is not much greater (14.8 Å) and reflects the average of the distances between each of the three pairs of tryptophans in this complex. Similar calculations on the 18-mer(u) (α181–198) alone indicate that the average distance between Trp-184 and Trp-187 was 14.3 ± 0.5 Å, consistent with peptide modeling studies.

Table IV: Solvent Accessibility of Tyrosyl Residues Determined by Second-Derivative Spectroscopy[a]

peptides	r_n[b]	r_u[c]	Tyr/Trp[d]	r_a[e]	α[f]
12-mer	0.77	0.79	2	0.3	0.95
18-mer(b)	1.1	1.3	2	0.3	0.80
18-mer(u)	0.72	0.89	2	0.3	0.71
32-mer	0.56	0.77	1.67	0.36	0.49
BGTX	0.45	0.76	2	0.3	0.38
12-mer + BGTX	0.47	0.72	2	0.3	0.40
18-mer(b) + BGTX	0.6	0.88	2	0.3	0.52
18-mer(u) + BGTX	0.52	0.82	2	0.3	0.42
32-mer + BGTX	0.43	0.58	1.75	0.33	0.46

[a] The parameter (r) was determined by second-derivative spectroscopy as described under Materials and Methods. [b] Determined in 0.05 M phosphate buffer, pH 7.4. [c] Determined in 6.0 M Gdn-HCl in 0.05 M phosphate, pH 6.5. [d] Ratio calculated from amino acid composition. [e] Values for Tyr/Trp ratios taken from Ragone et al. (1984). [f] $\alpha = (r_n - r_a)/(r_u - r_a)$.

Second-Derivative Spectroscopy. Since the fluorescence emission of tyrosine is relatively insensitive to environmental or solvent effects, it has been suggested that second-derivative absorption spectroscopy may yield more useful information concerning the solvent accessibility of the phenol rings (Ragone et al., 1984). The data in Table IV describe the solvent exposure of the tyrosyl residues in the peptide and the peptide–BGTX complexes in terms of the parameter α, which is defined as the relative percent exposure of tyrosines to solvent. It appears that both tyrosines in the dodecamer (α185–196) are nearly fully exposed to the aqueous solvent. In the 18-mer (α181–198) peptides, the tyrosines seem to be partially sequestered since α is reduced to a value of 80% for 18-mer(b) (α181–198) and 70% for 18-mer(u) (α181–198). For comparison, the two tyrosines in BGTX have a relative exposure of 38% while the corresponding value for the 32-mer (α173–204) is 49%. In the nAChR-derived peptide fragments, the percent exposure of tyrosine to solvent thus appears to decrease with increasing chain length. In all of the complexes, however, α appears to be similar (α = 0.40–0.52). By comparing the α values for free vs bound peptides, it appears that, in general, tyrosines become less accessible to solvent upon complex formation with BGTX (Table IV).

Discussion

From the intrinsic fluorescence studies of the nAChR-derived peptide fragments, the comparison of the spectral parameters (λ_{max} and Φ) for the peptide tryptophan residues suggests that the level of ordered structure surrounding the tryoptophan residues increases with increasing chain length. In addition, at neutral pH, there is a significant difference in the tryptophan environment for two of the peptides differing only in terminal charge [18-mer(b) (α181–198) and 18-mer(u) (α181–198)]. The 18-mer(u) (α181–198) with the two additional terminal charged groups appears to provide a much more hydrophobic environment for the tryptophan side chain perhaps through the induction of hydrophobic clustering. At low pH, however, the spectral properties (Table II) of these two peptides are very similar. Energy-transfer experiments support the view that the structure of the 18-mer(b) (α181–198) peptide differs significantly from the 18-mer(u) (α181–198) peptide. Whereas in all the other peptides the effective average distance r between tyrosine and tryptophan is in the range of 6.6–7.6 Å, in the case of the 18-mer(b) (α181–198)

peptide, r = 11.7 Å. The larger value for r may suggest a more extended conformation in comparison to the 18-mer(u) (α181–198) peptide. The second-derivative spectroscopy based investigation of the environment of the tyrosine residues in the peptides supports this view. The tyrosine residues in the 18-mer(b) (α181–198) peptide appear to be more accessible to solvent than those in the 18-mer(u) (α181–198) peptide. In general, the solvent accessibility of the tyrosine residues decreased with increasing chain length in the nAChR-derived peptide fragments (Table IV).

The investigation of tyrosine fluorescence also reveals some potentially interesting structural features in these peptides. The observed tyrosine emission with a λ_{max} at 330 nm is suggestive of either a ground-state tyrosinate or an excited-state tyrosinate resulting from a strongly hydrogen-bonded ground-state tyrosine as suggested by Szabo et al. (1978). The absorption spectra failed to reveal any ground-state tyrosinate or tyrosine excimer formation. Such ground-state phenomena would be expected to give rise to a corresponding red shift in the absorption spectrum (Wetlaufer, 1962). We therefore conclude that the unusual tyrosine fluorescence is due to excited-state tyrosinate formation. In support of this, we observe that the red-shifted tyrosine fluorescence is abolished by low pH or guanidine denaturation. Both of these treatments would be expected to eliminate tyrosinate fluorescence if it were due to hydrogen bonding (Prendergast et al., 1984).

Rayner et al. (1978) have shown that the phenolic hydroxyl of tyrosine can undergo excited-state proton transfer when a suitable proton acceptor is present. This phenomenon has also been observed in a number of polypeptides (Longworth, 1981). Although the nAChR-derived peptides vary considerably in the amount of tyrosinate fluorescence emission, in every case, the fluorescence of the peptide–BGTX complex indicates the presence of significant tyrosinate fluorescence (discussed below). The proton acceptor responsible for tyrosinate production is unknown but could be provided by the highly conserved histidine side chain in the nAChR peptide fragments or by a backbone carbonyl. It is also possible that a tyrosine in BGTX may be responsible for the observed tyrosinate fluorescence in the complexes.

In all cases examined here, the binding of the nAChR-derived peptide fragments to BGTX results in a net increase in total fluorescence accompanied by a blue shift in the tryptophan fluorescence maximum. In contrast, it has been reported that the binding of a 13-mer peptide, (α179–191) (from either calf or human nAChR), to α-cobratoxin is accompanied by fluorescence quenching (Radding et al., 1988). We have also observed similar quenching upon binding of the dodecamer (α185–196) to α-cobratoxin (unpublished data), suggesting that sequence differences between α-cobratoxin and BGTX may underlie the difference in fluorescence behavior upon complex formation. Interestingly, although BGTX leads to enhanced fluorescence upon binding to native receptor, the binding of α-cobratoxin to the native receptor leads to a decrease in fluorescence (Endo et al., 1986).

The binding of the nAChR-derived peptide fragments to BGTX follows a relatively long time course (Figure 5). In solid-phase assays, an extended time course was also observed (Wilson et al., 1988). The apparently slow rate of complex formation suggests that binding involves multiple-state rearrangements prior to equilibration at the most stable configuration. This hypothesis is supported by ^{1}H NMR experiments of the complex formed between the 18-mer(b) (α181–198) and BGTX at various temperatures (Hawrot et al., 1990). From these studies and other NMR experiments measuring the time course of complex formation (unpublished data), it is clear that, prior to final equilibration, a number of conformers of the complex can coexist in slow exchange.

The observed fluorescence enhancement upon binding may be due to a number of factors. Enhancement could be due to a combination of (1) a change in environment of any of the fluorescent residues in either the peptide or the BGTX, (2) a relative decrease in the intrinsic quenching of the tryptophan fluorescence in native BGTX, (3) increased tyrosinate formation, and (4) resonance energy-transfer mechanisms. Since there is a significant blue shift in λ_{max} upon complex formation, at least some of the enhancement appears to be due to a change in environment of tryptophan residues. In addition, it is clear that the fluorescence quantum yield of BGTX (Φ = 0.036) is low in comparison to other polypeptides including another related neurotoxin, neurotoxin I from *Naja haje*, where Φ = 0.075 (Chicheportiche et al., 1972). The quantum yield of BGTX at pH 2.9 is increased relative to pH 7 (Chen et al., 1982), suggesting that the fluorescence of the single tryptophan in BGTX is normally quenched at neutral pH. It is possible, therefore, that binding to the peptide fragments leads to a change in the environment of the BGTX tryptophan that may relieve some of this quenching. Our studies also show that an excited-state tyrosinate is common to all the peptide–BGTX complexes (Figure 7) and thus also appears to contribute to the observed enhanced fluorescence. The electronegativity of a hydrogen-bonded tyrosine hydroxyl may be a structural characteristic of functional importance for binding and ligand recognition in the native nAChR. Since a negative subsite is presumed to be located within the nAChR binding site (Kao et al., 1984; Endo et al., 1986; Dennis et al., 1988b), a partial negative charge provided by tyrosine may contribute significantly to the coordination of the positive charge on the tertiary amine found in acetylcholine and other nicotinic agonists (Abramson et al., 1989; Pearce & Hawrot, 1990). We have recently prepared modified peptide fragments containing a Phe in place of the tyrosine at position 190 of the α-subunit. In support of the proposed role of tyrosine in binding recognition, we found that these selectively modified peptide fragments showed greatly reduced ability to bind BGTX (Pearce et al., 1990).

Since the dodecamer (α185–196)–BGTX complex contains only two tryptophan residues, one in each of the two polypeptides, we decided to use energy transfer between the tryptophan residues to calculate the Förster distance between the side chains in the bound complex. From the calculation of J_{AD} and R_0 by the graphical method, the distance between the two tryptophan residues is approximately 11.5 Å. This distance is apparently incompatible with any model that predicts that Trp–Trp stacking is involved in binding recognition and should provide a useful distance constraint for future model building of the complex. Additional intermolecular distance constraints are being obtained from two-dimensional NOESY ^{1}H NMR experiments of the dodecamer (α185–196)–BGTX complex (Basus and Hawrot, unpublished experiments).

Aside from the structural information that can be obtained from intrinsic fluorescence measurements, fluorescence changes observed upon binding form the basis for very convenient solution assays of binding under various experimental conditions (Radding et al., 1988; Shi et al., 1988; Pearce & Hawrot, 1989). Most peptide–BGTX binding assays had previously relied on solid-phase attachment for the separation of bound and free ligand (Neumann et al., 1986a; Wilson et al., 1988). In the fluorescence assays, the calculated K_ds for

the dodecamer (α185–196) and 18-mer (α181–198) were 1.0 ± 0.3 and 0.33 ± 0.1 μM, respectively. In the case of the dodecamer (α185–196), the binding affinity was constant over a large pH range varying from pH 2 to pH 9. Since there was no pH dependence for the λ_{max} of the fluorescence, it appears that there is very little change in the structure of the complex in this pH range. The apparent affinities obtained here for the nAChR-derived peptide fragments compare favorably with the estimates of peptide-binding affinities obtained with other procedures (Neumann et al., 1986b; Wilson et al., 1988; Radding et al., 1988; Aronheim et al., 1988).

In conclusion, our fluorescence studies of a number of nAChR-derived peptide fragments that retain the ability to bind BGTX show that (1) the quantum yield of tyrosine and tryptophan decreases with increasing chain length, (2) the λ_{max} of the tryptophan intrinsic fluorescence of these peptides undergoes a significant blue shift with increasing chain length, suggesting an increase in the hydrophobicity of the tryptophan environment, (3) the observation of an excited-state tyrosinate fluorescence is a common characteristic for the peptide–BGTX complexes, (4) in all cases, binding of BGTX to these peptide fragments is accompanied by enhanced fluorescence and a blue shift of the λ_{max}, (5) the enhanced fluorescence upon binding provides a basis for a solution-phase assay from which affinity constants can be readily obtained, and (6) the average effective distance between the Trp-187 in the dodecamer (α185–196) and Trp-28 in BGTX is 11.5 Å based on energy-transfer calculations. These studies provide the groundwork for future biophysical investigations of agonist interactions with receptor-derived peptide fragments. Further study of the interaction of the nAChR-derived peptide fragments with BGTX should contribute to the elucidation of the mechanisms underlying the interaction of BGTX with structural determinants within the binding site of the native receptor.

References

Abramson, S. N., Li, Y., Culver, P., & Taylor, P. (1989) *J. Biol. Chem. 264*, 12666–12672.

Albert, A., & Serjeant, E. P. (1971) in *The Determination of Ionization Constants*, Chapman and Hall, Ltd., London.

Aronheim, A., Eshel, Y., Mosckovitz, R., & Gershoni, J. M. (1988) *J. Biol. Chem. 263*, 9933–9937.

Barkas, T., Mauron, A., Roth, B., Alliod, C., Tzartos, S. J., & Ballivet, M. (1987) *Science 235*, 77–80.

Barrantes, F. J. (1978) *J. Mol. Biol. 124*, 1–26.

Becker, R. (1969) in *Theory and Interpretation of Fluorescence*, pp 239–244, Wiley Interscience, New York.

Birks, J. B. (1970) in *Photophysics of Aromatic Molecules*, Wiley Interscience, New York.

Bonner, R., Barrantes, F. J., & Jovin, T. M. (1976) *Nature (London) 263*, 429–431.

Changeux, J. P., Devilliers-Thiery, A., & Chemoulli, P. (1984) *Science 225*, 1335–1345.

Chen, Y.-H., Tai, J.-C., Huang, W.-J., Lai, M.-Z., Hung, M.-C., Lai, M.-D., & Yang, J. T. (1982) *Biochemistry 21*, 2592–2600.

Chicheportiche, R., Rochat, C., Sampieri, F., & Lazdunski, M. (1972) *Biochemistry 11*, 1681–1691.

Cohen, J. B., & Changeux, J. P. (1975) *Annu. Rev. Pharmacol. 15*, 83–103.

Cowgill, R. W. (1963) *Arch. Biochem. Biophys. 100*, 36–37.

Dennis, M., Giraudat, J., Kotzyba-Hibert, F., Goeldner, M., Hirth, C., Chang, J.-Y., & Changeux, J.-P. (1986) *FEBS Lett. 207*, 243–249.

Dennis, M., Giraudat, J., Kotzyba-Hibert, F., Goeldner, M., Hirth, C., Chang, J.-Y., Lazure, C., Chretien, M., & Changeux, J.-P. (1988) *Biochemistry 27*, 2346–2357.

Donovan, J. W. (1969) in *Physical Principles and Techniques of Protein Chemistry* (Leach, S. J., Ed.) Part A, pp 101–170, Academic Press, New York.

Eldefrawi, M. E., & Eldefrawi, A. T. (1977) *Recept. Recognit., Ser. A 4*, 197–258.

Eisinger, J. (1969) *Biochemistry 8*, 3902–3907.

Eisinger, J., Feuer, B., & Lamola, A. A. (1969) *Biochemistry 8*, 3908–3914.

Endo, T., Nakanishi, M., Furukawa, S., Joubert, F., Tamiya, N., & Hayashi, K. (1986) *Biochemistry 25*, 395–404.

Fairclough, R. H., & Cantor, C. R. (1978) *Methods Enzymol. 28*, 347–352.

Förster, Th. (1966) *Modern Quantum Chemistry*, Istanbul Lectures, Academic Press, New York.

Fraenkel, Y., Navon, G., Aronheim, A., & Gershoni, J. M. (1989) *Biophys. J. 55*, 66a.

Hawrot, E., Colson, K. L., Armitage, I. M., & Song, G.-Q. (1990) in *Frontiers of NMR in Molecular Biology*, pp 27–36, Alan R. Liss, Inc., New York.

Heidmann, T., & Changeux, J. P. (1978) *Annu. Rev. Biochem. 47*, 317–357.

Kaneda, N., Tanaka, F., Kohno, M., Hayashi, K., & Yagi, K. (1982) *Arch. Biochem. Biophys. 218*, 376–383.

Kao, P. N., Dwork, A. J., Kaldany, R. R.-J., Silver, M. L., Wideman, J., Stein, S., & Karlin, A. (1984) *J. Biol. Chem. 259*, 11662–11665.

Karlin, A. (1980) *Cell Surf. Rev. 6*, 191–260.

Karlsson, E. (1979) *Handb. Exp. Pharmacol. 52*, 159–212.

Kronman, M. J., & Holmes, L. G. (1971) *Photochem. Photobiol. 14*, 113–134.

Lehrer, S. S., & Fasman, G. D. (1967) *Biochemistry 6*, 757–767.

Longworth, J. W. (1971) in *Excited States of Proteins and Nucleic Acids* (Steiner, R. F., & Weinryb, I., Eds.) pp 319–483, Plenum, New York.

Longworth, J. W. (1981) *Ann. N.Y. Acad. Sci. 366*, 237–245.

Maksimov, M. Z., & Rozman, I. M. (1968) *Opt. Spectrosc. (Engl. Transl.) 1*, 168.

Malencik, D. A., & Anderson, S. R. (1987) *Biochemistry 26*, 695–704.

McCarthy, M. P., & Stroud, R. M. (1989) *Biochemistry 28*, 40–48.

Menez, A., Montenay-Garestier, T., Fromagest, P., & Helene, C. (1980) *Biochemistry 19*, 5202–5208.

Mulac-Jericevic, B., & Atassi, M. Z. (1986) *FEBS Lett. 199*, 68–74.

Neumann, D., Gershoni, J. M., Fridkin, M., & Fuchs, S. (1985) *Proc. Natl. Acad. Sci. U.S.A. 82*, 3490–3493.

Neumann, D., Barchan, D., Fridkin, M., & Fuchs, S. (1986a) *Proc. Natl. Acad. Sci. U.S.A. 83*, 9250–9253.

Neumann, D., Barchan, D., Safran, A., Gershoni, J. M., & Fuchs, S. (1986b) *Proc. Natl. Acad. Sci. U.S.A. 83*, 3008–3011.

Oblas, B., Singer, R. H., & Boyd, N. H. (1986) *Mol. Pharmacol. 29*, 649–656.

Parker, C. A., & Rees, W. T. (1966) *Analyst 85*, 587–592.

Pearce, S. F. A., & Hawrot, E. (1989) *Biophys. J. 55*, 517a.

Pearce, S. F. A., & Hawrot, E. (1990) *Biophys. J. 57*, 443a.

Pearce, S. F. A., Preston-Hurlburt, P., & Hawrot, E. (1990) *Proc. R. Soc. London, B 241*, 207–213.

Pederson, S. E., Dreyer, E. B., & Cohen, J. B. (1986) *J. Biol. Chem. 261*, 13735–13743.

Prendergast, F. G., Hampton, P. D., & Jones, B. (1984) *Biochemistry 23*, 6690–6697.

Radding, W., Corfield, P. W. R., Levinson, L. S., Hashim, G. A., & Low, B. W. (1988) *FEBS Lett. 231*, 212–216.
Ragone, R., Colonna, G., Balestrieri, C., Servillo, L., & Irace, G. (1984) *Biochemistry 23*, 1871–1875.
Ralston, S., Sarin, V., Thanh, H. L., Rivier, J., Fox, J. L., & Lindstrom, J. (1987) *Biochemistry 26*, 3261–3266.
Rayner, D. M., Krajcarski, T., & Szabo, A. G. (1977) *Can. J. Chem. 56*, 1238–1245.
Saito, Y., Tachibana, H., & Hayashi, H. (1981) *Photochem. Photobiol. 33*, 289–295.
Shi, Q., Colson, K. L., Lentz, T. L., Armitage, I. M., & Hawrot, E. (1988) *Biophys. J. 53*, 94a.
Steinberg, I. Z. (1968) *J. Chem. Phys. 48*, 2411–2415.
Stryer, L. (1966) *J. Am. Chem. Soc 88*, 5708–5712.
Stryer, L. (1978) *Annu. Rev. Biochem. 47*, 819–846.
Szabo, A., Lynn, K. R., Krajcarski, D. T., & Rayner, D. M. (1978) *FEBS Lett. 94*, 249–252.
Tao, T., Lamkin, M., & Lehrer, S. (1983) *Biochemistry 22*, 3059–3066.
Teale, F. W. J., & Weber, G. (1957) *Biochem. J. 65*, 476–482.
Weber, G., & Young, L. B. (1964) *J. Biol. Chem 239*, 1424–1430.
Weber, G., Borris, D. P., De Robertis, E., Barrantes, F. J., La Torre, J. L., & De Carlin, M. C. L. (1971) *Mol. Pharmacol. 7*, 530–537.
Weinberg, R. B. (1988) *Biochemistry 27*, 1515–1521.
Wetlaufer, D. B. (1962) *Adv. Protein Chem. 17*, 303–390.
Wilson, P. T., Lentz, T. L., & Hawrot, E. (1985) *Proc. Natl. Acad. Sci. U.S.A. 82*, 8790–8794.
Wilson, P. T., Hawrot, E. & Lentz, T. L. (1988) *Mol. Pharmacol. 34*, 643–650.

The Membrane-Bound Domain of the Phosphotransferase Enzyme II^{mtl} of *Escherichia coli* Constitutes a Mannitol Translocating Unit†

Juke S. Lolkema, Dolf Swaving Dijkstra, Ria H. ten Hoeve-Duurkens, and George T. Robillard*
Department of Physical Chemistry and Institute BIOSON, Nijenborgh 16, 9747 AG Groningen, The Netherlands
Received April 18, 1990; Revised Manuscript Received June 26, 1990

ABSTRACT: The orientation of the mannitol binding site on the *Escherichia coli* phosphotransferase enzyme II^{mtl} in the unphosphorylated state has been investigated by measuring mannitol binding to cytoplasmic membrane vesicles with a right-side-out and inside-out orientation. Enzyme II^{mtl} is shown to catalyze facilitated diffusion of mannitol at a low rate. At equilibrium, bound mannitol is situated at the periplasmic side of the membrane. The apparent binding constant is 40 nM for the intact membranes. Solubilization of the membranes in detergent decreases the affinity by about a factor of 2. Inside-out membrane vesicles, treated with trypsin to remove the C-terminal cytoplasmic domain of enzyme II^{mtl}, showed identical activities. These experiments indicate that the translocation of mannitol is catalyzed by the membrane-bound N-terminal half of enzyme II^{mtl} which is a structurally stable domain.

The mannitol-specific transport protein enzyme II^{mtl} [for reviews, see Postma and Lengeler (1985) and Robillard and Lolkema (1988)][1] catalyzes mannitol transport and phosphorylation via the following reaction in which P-enolpyruvate serves as the initial phosphoryl group donor.

$$\text{mannitol}_{out} + \text{P-HPr} \xrightarrow{II^{mtl}} \text{mannitol-P}_{in} + \text{HPr}$$

Phosphorylated enzyme II^{mtl} is an intermediate in this reaction. Enzyme II^{mtl} is a 68-kDa polypeptide chain for which the primary sequence has been deduced from the base sequence of the cloned mtlA gene (Lee & Saier, 1983). Hydropathy analysis divides the protein into a hydrophobic N-terminal half and a hydrophilic C-terminal half. This is in agreement with topographical studies that demonstrate that half of the enzyme is globular and situated at the cytoplasmic side of the membrane whereas the other half is integrated in the membrane (Stephan & Jacobson, 1986). The latter is assumed to be responsible for the translocation of the solute. The hydrophilic C-terminal half consists of two separate domains that have been subcloned from the mtlA gene and shown to be functional in complementation assays (van Weeghel et al., 1990; White & Jacobson, 1990). Each of these two domains contains a phosphorylation site. His554 accepts the phosphoryl group from P-Hpr and passes it on, via an intramolecular transfer, to Cys384 in the second domain. Phosphorylated Cys384 is the donor for the incoming sugar (Pas & Robillard, 1988).

A high-affinity mannitol binding site on the unphosphorylated enzyme has been demonstrated with purified enzyme II^{mtl} by ultrafiltration (Pas et al., 1988). Data have been presented showing that the site is localized in the N-terminal half of the protein (Grisafi et al., 1989). The present study focuses on the orientation of the binding site on enzyme II^{mtl} with respect to the two sides of the membrane. The binding of mannitol was measured to membrane vesicles with a right-side out (RSO) or an inside-out (ISO) orientation.

Experimental Procedures

Materials

D-[1-^{3}H(N)]Mannitol (706.7 GBq/mmol) was purchased from NEN Research Products. Decylpoly(ethylene glycol) 300 (decylPEG) was synthesized by B. Kwant in our labora-

† This work was supported by the Netherlands Foundation for Chemical Research (SON) with financial aid from the Netherlands Organization for Scientific Research (NWO).
* To whom correspondence should be addressed.

[1] Abbreviations: ISO, inside-out; RSO, right-side-out; DTT, dithiothreitol; decylPEG, decylpoly(ethylene glycol) 300; mtl, mannitol.

0006-2960/90/0429-10659$02.50/0